

Keck Spectroscopy and NICMOS Photometry of a Redshift

$z = 5.60$ **Galaxy**¹

Ray J. Weymann^{2,3}

E-mail: rjw@ociw.edu

Daniel Stern⁴, Andrew Bunker⁴, Hyron Spinrad⁴

E-mail: dstern,abunker,hspinrad@bigz.berkeley.edu

Frederic H. Chaffee⁵

E-mail: fchaffee@keck.hawaii.edu

Rodger I. Thompson⁶

E-mail: thompson@as.arizona.edu

and

Lisa J. Storrie-Lombardi³

E-mail: lisa@ociw.edu

[to appear in the Astrophysical Journal Letters]

Received _____; accepted _____

¹ Optical data presented herein were obtained at the W.M. Keck Observatory, which is operated as a scientific partnership among the California Institute of Technology, the University of California and the National Aeronautics and Space Administration. The Observatory was made possible by the generous financial support of the W.M. Keck Foundation. The near-infrared observations were obtained with the Near-Infrared Camera and Multi-Object Spectrometer on the NASA/ESA Hubble Space Telescope which is operated by AURA Inc., under contract with NASA.

²Visiting Prof., Lick Observatory, Santa Cruz, CA 95064

³Observatories of the Carnegie Institution of Washington, 813 Santa Barbara Street, Pasadena, CA 91101

⁴Astronomy Dept., 601 Campbell Hall, U. C. Berkeley, Berkeley, CA 94720

⁵W. M. Keck Observatory, 65-1120 Mamalahoa Hwy., Kamuela, HI 96743

⁶Steward Observatory, The University of Arizona, Tucson, AZ 85721

ABSTRACT

We present Keck LRIS spectroscopy along with NICMOS F110W (\sim J) and F160W (\sim H) images of the galaxy HDF 4–473.0 (hereafter 4-473) in the Hubble Deep Field, with a detection of an emission line consistent with Ly- α at a redshift of $z = 5.60$. Attention to this object as a high redshift galaxy was first drawn by Lanzetta, Yahil and Fernandez-Soto and appeared in their initial list of galaxies with redshifts estimated from the WFPC2 HDF photometry. It was selected by us for spectroscopic observation, along with others in the Hubble Deep Field, on the basis of the NICMOS F110W and F160W and WFPC2 photometry. For $H_0 = 65 \text{ km s}^{-1} \text{ Mpc}^{-1}$ and $q_0 = 0.125$, use of simple evolutionary models along with the F814W (\sim I), F110W, and F160W magnitudes allow us to estimate the star formation rate ($\sim 13M_{\odot}/\text{yr}$). The colors suggest a reddening of $E(B-V) \sim 0.06$. The measured flux in the Ly- α line is approximately $1.0 \times 10^{-17} \text{ ergs cm}^{-2} \text{ s}^{-1}$ and the restframe equivalent width, correcting for the absorption caused by intervening H I, is approximately 90 \AA . The galaxy is compact and regular, but resolved, with an observed FWHM of $\sim 0.44''$. Simple evolutionary models can accurately reproduce the colors and these models predict the Ly- α flux to within a factor of 2. Using this object as a template shifted to higher redshifts, we calculate the magnitudes through the F814W and two NICMOS passbands for galaxies at redshifts $6 < z < 10$.

Subject headings: cosmology: early universe – galaxies: formation – galaxies: evolution – galaxies: distances and redshifts

1. Introduction

There have recently been several programs aimed at discovering galaxies at very high redshifts, utilizing the strong effects on broadband colors arising from the Ly- α forest and Lyman continuum absorption, (Lanzetta *et al.* 1996; Madau *et al.* 1996; Steidel *et al.* 1996; Spinrad *et al.* 1998; Fernandez-Soto *et al.* 1998), imaging to detect Ly- α emission through narrow band filters (Hu *et al.* 1998), Fabry Perot imaging (Thommes *et al.* 1998), long slit “serendipitous” Ly- α searches (Dey *et al.* 1998; Hu *et al.* 1988), and slitless spectroscopic searches (Lanzetta 1998). The ability of the HST NICMOS (Thompson *et al.* 1998a) to obtain very deep images over the range 0.8μ to 1.8μ offers an additional tool for discovering faint high redshift candidates. We report here the detection of the first such galaxy incorporating this NICMOS data, and describe some of its properties.

2. Target Selection, NICMOS Images and Photometry

During the first NICMOS Camera 3 HST Campaign in January 1998, very deep images were taken of a portion of the WFPC2 HDF Chip 4 in both the F110W and F160W filters, corresponding approximately to the J and H bands. A catalog of the galaxies found on these images and discussion of the contents of this catalog is presented elsewhere (Thompson *et al.* 1998b). Preliminary inspection of these images revealed that the galaxy 4-473 in the Williams *et al.* (1996) catalog was relatively bright in F110W and F160W, distinctly fainter in the F814W (I) band and not visible in F606W (V). Although we were unaware of it at the time, this object had already been noted by Lanzetta, Yahil & Fernández-Soto (1996) as a high redshift candidate, with a photometrically estimated redshift from the F814W and F606W images of 6.8. The negative F110W–F160W (AB) NICMOS color, together with the moderately red (positive) F814W–F110W AB color made it a very strong candidate for spectroscopic observations to confirm it as a high redshift galaxy. Indeed, combined with its

non-detection in KPNO IRIM IR imaging (Dickinson *et al.* 1998) the revised photometric redshift of 5.64 by Fernández-Soto, Lanzetta & Yahil 1998 is remarkably close to what we have observed spectroscopically.

To measure colors on a consistent basis, we have measured 1.0'' diameter aperture magnitudes (AB scale used throughout) and obtain values of 27.12 ± 0.19 in F814W, 26.64 ± 0.04 in F110W and 26.86 ± 0.04 in F160W. The S/N of the corresponding F606W image is < 1 , and the lower limit on the F606W - F814W color is 2.31 from Williams *et al.* (1996). A mosaic of $3'' \times 3''$ regions around 4-473 in these 4 passbands is shown in Figure 1.

3. Spectroscopic Observations of 4-473

Although 4-473 is extremely faint, recent successes in detecting Ly- α emission from very high redshift galaxies (Dey *et al.* 1998; Hu *et al.* 1998) encouraged us to attempt spectroscopic observations. Accordingly we observed the HDF on 25 February 1998 UT using the slitmask spectroscopic mode of the Low Resolution Imaging Spectrometer (LRIS; Oke *et al.* 1995) at the Cassegrain focus of the Keck II Telescope. The 1.5'' wide slitlet containing 4-473 was $\approx 24''$ long, allowing for effective sky removal. The observations were made with the 400 l/mm grating ($\lambda_{\text{blaze}} \approx 8500 \text{ \AA}$; $\Delta\lambda \approx 11 \text{ \AA}$). The telescope was offset 2.5'' along the slit between each 1800 second exposure to facilitate removal of the fringing in the near-IR regions of the spectrogram. A total of 9000 seconds of integration was obtained, and the reduced spectrogram revealed a faint emission line at $\approx 8030 \text{ \AA}$ at the position of 4-473 on the slitlet. We therefore reobserved 4-473 for an additional 5400 seconds on 27 June 1998 UT with LRIS in longslit mode, utilizing the relatively bright star HDF 4-454.0 at the center of HDF chip 4 as a control for both spectrophotometry and spectroastrometry. These observations were obtained with a 1'' slit and the 400 l/mm grating and confirmed the emission line detected in February.

Data reductions were performed using the *IRAF* package and followed standard slit spectroscopy procedures. Wavelength calibration was performed using a NeAr lamp, employing telluric lines to adjust the zero-point. Flux calibration employed a sensitivity function derived from 20,21 January 1998 UT observations of G191B2B and HZ 44 (Massey *et al.* 1988; Massey & Gronwall 1990) and was adjusted to ensure F814W magnitudes derived from spectrophotometry of the brighter serendipitous objects HDF 4–460.0 (February 1998 data) and HDF 4–454.0 (June 1998 data) matched the Williams *et al.* (1996) imaging photometry. Our composite spectrogram, presented in Fig. 2, reveals a robust detection of an emission line at 8029 \AA with an integrated flux of $\approx 1.0 \times 10^{-17} \text{ ergs cm}^{-2} \text{ s}^{-1}$.

4. Identification of the Emission Line as Ly- α

As discussed below, we believe the only reasonable identification for the emission line in 4-473 is Ly- α . Other possible alternatives are H α , [O III] 5007, and [O II] 3727; [O III] 4960 or H β are unlikely since [O III] 5007 would also be detected. (By chance, the slitlet for the February observations passed through the galaxy HDF 4–460.0, which has a redshift of $z \sim 0.68$ and has three lines at similar observed wavelengths as the line in 4-473.) If the line were H α , the restframe colors of 4-473 would be unlike any galaxy of which we are aware. Identification of the line as [O III] 5007 itself might be possible since the corresponding [O III] 4960 and H β lines would be weaker and in a region of strong OH night sky emission, but the corresponding [O II]3727 would fall in a region uncontaminated by night sky emission and is not present to a very low flux level. By contrast, the [O II] 3727 line in the spectrum of HDF 4–460.0 is readily observed and is very strong.

The colors may also be used to rule out with high probability an identification as [O II] 3727. To make this latter statement quantitative we have used the 6 template spectra of

star-forming galaxies assembled by Calzetti *et al.* (1994). These templates are each sets of star-forming galaxies observed with both IUE and from the ground, and grouped into 6 sets characterized by different amounts of internal reddening.⁷ Shifting these templates to the redshift implied if the line were identified as [O II] 3727, the F606W - F814W colors range from 0.39 to 0.79, *i.e.*, much *bluer* than the observed limit of > 2.31 . Moreover, for the reddest of the templates, the F814W–F110W and F110W–F160W colors are much *redder* than the observed colors: 0.79 and 0.64 compared to the observed values of +0.48 and -0.22, respectively. Galaxies with old stellar populations, in which a hidden source of ionizing radiation might produce the [O II] 3727 emission encounter similar difficulties.

An additional argument in favor of the Ly- α identification comes from the profile of the line itself. As seen in Figure 2, the line is asymmetric, with absorption on the blue side, just as anticipated from absorption by local H I and/or a dense Ly- α forest (cf. Dey *et al.* 1998). In the following we assume therefore that the Ly- α identification is correct, and the wavelength at the peak of the line emission implies a redshift of 5.603 ± 0.002 .

5. Discussion

HDF 4–473 is not the galaxy with the highest reported redshift. A galaxy of slightly higher redshift has been reported in a serendipitous long slit exposure by Hu *et al.* (1998), and no doubt more high redshift galaxies will be forthcoming from the various approaches described in the Introduction (cf. Lanzetta 1998). However, the combination of the WFPC2 and NICMOS images allow us to make some estimates of the star formation rate as well as the reddening.

⁷We thank Dr. Calzetti for kindly making available these templates to us in digital form.

5.1. Empirical Estimate of Continuum Level and Slope

We have been unable to detect a continuum in our spectroscopic observations, since only a fairly limited portion of the spectrum redward of Ly- α is free of strong OH emission. To estimate the continuum level we use a semi-empirical model in which we assume a power law of the form

$$F(\lambda) = F_0 \times (\lambda/1.6\mu)^\beta$$

and impose the absorption due to the Ly- α forest and Ly- α continuum calculated recently by Madau, Pozzetti & Dickinson (1998). We then determine the values of F_0 and β as well the flux in the Ly- α emission line from the F160W, F110W and F814W magnitudes. We regard the flux in the Ly- α emission line as a parameter to be determined since our absolute flux measurement is somewhat uncertain and the Ly- α flux makes a significant contribution to the total counts in the F814W filter. The magnitudes are very accurately reproduced for this redshift with $\beta = -2.40$, a Ly- α flux of 1.2×10^{-17} ergs cm $^{-2}$ s $^{-1}$ and a continuum flux at the Ly- α line of 4.0×10^{-20} ergs cm $^{-2}$ s $^{-1}$ Å $^{-1}$. This implies a restframe equivalent width of about 45 Å for the unobscured portion of the line, and about 90 Å if, as appears to be the case from the line profile, half of the line is absorbed away.

5.2. Evolutionary Models, Star Formation Rate and Reddening

We construct evolutionary models as follows: 1) We use the latest version of the GISSEL model (Bruzual & Charlot 1993; Leitherer *et al.* 1996) for a Salpeter IMF and $125M_\odot$ upper limit cutoff. 2) The Madau *et al.* (1998) Lyman absorption model is used. 3) We use the Calzetti *et al.* (1994) reddening law in which we have set the ratio, R, of reddening to extinction to 3.1. 4) We assume a constant rate of star formation extending from the observed epoch over some period δT years. 5) We fix the flux of Ly- α at

1.2×10^{-17} ergs $\text{cm}^{-2} \text{s}^{-1}$ on the basis of the semi-empirical determination above. 6) We adopt the cosmological parameters $H_0 = 65 \text{ km s}^{-1} \text{ Mpc}^{-1}$ and $q_0 = 0.125$.

We have explored models in which we vary the reddening (characterized by $E(B-V)$), the rate of star formation, and the duration of the star formation epoch, δT . For a given reddening and star formation duration, we adjust the star formation rate to force agreement with the F160W magnitude. The resultant F110W–F160W and F814W–F110W colors are rather insensitive to the star formation duration, and even the inferred star formation rate is not strongly dependent upon δT over the range $20 < \delta T < 80$ Myr. We adopt in the following $\delta T = 5 \times 10^7$ years. The F110W–F160W and F814W–F110W colors can be exactly matched with $E(B-V) = 0.06$, and a star formation rate of $13M_\odot/\text{yr}$.

Estimates on the limits for the reddening and corresponding star formation rates are approximately $E(B-V) \sim 0.00$, and $\text{SFR} \sim 8M_\odot/\text{yr}$ and $E(B-V) \sim 0.12$ and $\text{SFR} \sim 19M_\odot/\text{yr}$. These reddening and star formation rate estimates are somewhat lower than those recently obtained for galaxies at $z = 5.34$ and $z = 4.92$ by Armus *et al.* (1998) and Soifer *et al.* (1998). At a wavelength of $\lambda 9900\text{\AA}$, corresponding to a rest wavelength of $\lambda 1500\text{\AA}$, the model predicts a flux of 2.6×10^{-20} ergs $\text{cm}^{-2} \text{s}^{-1} \text{\AA}^{-1}$. Correcting for the extinction, our adopted cosmological model implies a luminosity of 1.4×10^{41} ergs $\text{sec}^{-1} \text{\AA}^{-1}$, which agrees well with the relation between star formation rate and UV luminosity proposed by Madau, Pozzetti & Dickinson (1998). For a cosmology with $H_0 = 50 \text{ km s}^{-1} \text{ Mpc}^{-1}$ and $q_0=0.5$ the corresponding luminosity would be lower by a factor of 1.8. We do not, of course, claim that these model properties are well determined, given all the uncertainties inherent in the assumptions listed above. However, additional support comes from the *predicted* Ly- α flux. If subjected to the same reddening as the continuum and if 50% is absorbed (as seems reasonable based upon the asymmetric profile), this yields a flux of 1.8×10^{-17} ergs $\text{cm}^{-2} \text{s}^{-1}$, in rough agreement with that observed. The modest excess in the

predicted flux over our best estimate for the observed value can be ascribed to destruction by dust of the multiply scattered Ly- α and/or by variations in the IMF to which the Ly- α flux is moderately sensitive.

5.3. Morphology

Inspection of the HST images reveals that 4-473 has a regular, compact morphology. We note that the other $z > 5$ galaxies for which imaging exists either have multiple components (Spinrad *et al.* 1998) or are resolved even from the ground (Dey *et al.* 1998).

In F160W the galaxy has FWHM=0.44". Comparison with a PSF star shows that 4-473 is clearly resolved (FWHM_{PSF}=0.2") with a deconvolved half-light radius of 0.2" (1.4 kpc), comparable to that found for many of the $z \approx 3$ Lyman-break galaxies (Giavalisco *et al.* 1996). The major/minor axial ratio is measured to be $\frac{a}{b} = 1.15 \pm 0.04$ in F160W. Neither an exponential disk nor a de Vaucouleurs $r^{1/4}$ law fit the radial profile well. A two-component model suggests that the disk may dominate, as with other “spheroidal” objects in the HDF (Marleau & Simard 1998). The characteristic disk scale length is $r_0 \approx 2.4$ kpc.

There is a nearby brighter object, HDF 4-497.0, which Bunker *et al.* (1998) have shown to be a foreground system associated with the nearby Lyman-break galaxy, HDF 4-555.1 (“the Hot Dog” at $z = 2.80$, Steidel *et al.* 1996). There appears to be a diffuse structure between HDF 4-497.0 and 4-473, the nature of which is uncertain. As this feature is still visible in the F606W band, it is likely not part of the higher-redshift system.

5.4. Extrapolation to Higher Redshifts

Using the “best fit” model above for the star formation rate and reddening, we can then predict the magnitudes a galaxy like 4-473 would have at higher redshifts. A more complete discussion is given in Thompson *et al.* (1998b). For $H_0 = 65 \text{ km s}^{-1} \text{ Mpc}^{-1}$ and $q_0 = 0.125$ and keeping the inferred Ly- α luminosity fixed, we obtain the values in Table 1. For $H_0 = 50 \text{ km s}^{-1} \text{ Mpc}^{-1}$ and $q_0 = 0.5$, the decrease in brightness with increasing redshift is less than for the $H_0 = 65$ and $q_0 = 0.125$ cosmology assumed in Table 1. Relative to the magnitudes in Table 1 the galaxy would be 0.04 magnitudes brighter at $z = 6$ and 0.33 magnitudes brighter at $z = 10$. Evidently, near IR imaging with NICMOS is, and will continue to be, a powerful tool for the study of high redshift galaxies out to $z \sim 10$.

The near-infrared observations are supported by NASA grant NAG5-3042 to the NICMOS instrument definition team. RJW thanks the W.M. Keck Observatory and the Lick Observatory for their hospitality during the period when this work was carried out and P. McCarthy and D. Koo for useful discussions. AB and LJSJL gratefully acknowledge financial support from NICMOS postdoctoral positions.

REFERENCES

- Armus, L., Matthews, K., Neugebauer, G., & Soifer, B.T. 1998, ApJ, in press
- Bruzual, G.A. & Charlot., S. 1993, ApJ, 405, 538
- Bunker, A.J., Stern, D., Spinrad, H., Dey, A., Steidel, C., & Wolfe, A. 1998, in preparation
- Calzetti, D., Kinney, A.L., & Storchi-Bergmann, T. 1994, ApJ, 429, 582
- Dey, A., Spinrad, H., Stern, D., Graham, J.R., & Chaffee, F.H. 1998, ApJ, 498, L93
- Dickinson, M.E., *et al.* 1998, in preparation
- Giavalisco, M., Steidel, C., & Macchetto, D. 1996 ApJ, 470, 189
- Hu, E.M., Cowie, L.L., & McMahon, R.G. 1998, 502, L99
- Fernández-Soto, A., Lanzetta, K., & Yahil, A. 1998, ApJ, submitted
- Lanzetta, K., Yahil, A., & Fernández-Soto, A. 1996, Nature, 381, 759
- Lanzetta, K., 1998, in proceedings of the Xth Rencontres de Blois, ‘The Birth of Galaxies’,
June 28 - July 4 1998, Blois, France, in preparation
- Leitherer, C. *et al.* 1996, PASP, 108, 996
- Madau, P., Ferguson, H.C., Dickinson, M.E., Giavalisco, M., Steidel, C.C., and Fruchter, A.
1996, MNRAS, 283, 1388
- Madau, P., Pozzetti, L., and Dickinson, M. 1998, ApJ, 498, 106
- Massey, P., Strobel, K., Barnes, J.V., & Anderson, E. 1988, ApJ, 328, 315
- Massey, P. & Gronwall, C. 1990, ApJ, 358, 344

Oke, J.B., Cohen, J.G., Carr, M., Cromer, J., Dingizian, A., Harris, F.H., Labrecque, S.,
Lucinio, R., Schall, W., Epps H., and Miller, J. 1995, PASP, 107, 375

Marleau, F.R. & Simard, L. 1998, ApJ, in press

Soifer, B.T., Neugebauer, G., Franx, M., Matthews, K. & Illingworth, G. 1998, ApJ, in
press

Spinrad, H., Stern, D., Bunker, A., Lanzetta, K., Yahil, A., Pascarella, S. & Fernández-Soto,
A. 1998, in preparation

Steidel, C.C., Giavalisco, M., Pettini, M., Dickinson, M., and Adelberger, K. 1996, ApJ,
462, L17

Thommes, E., Meisenheimer, K., Fockenbrock, R., Hippelein, H., Roser, H.-J., & Beckwith,
S. 1998, MNRAS, 293, 6

Thompson, R.I., Rieke, M., Schneider, G., Hines, D., & Corbin, M. 1998a, ApJ, 492, L95

Thompson, R.I., *et al.* 1998b, in preparation

Williams, R. E., Blacker, B., Dickinson, M., Dixon, W.V., Ferguson, H.C., Fruchter, A.S.,
Giavalisco, M., Gilliland, R.L., Henry, I., Katsanis, R., Levay, Z., Lucas, R.A.,
McElroy, D.B., Petro, L., Postman, M. 1996, AJ, 112, 1335

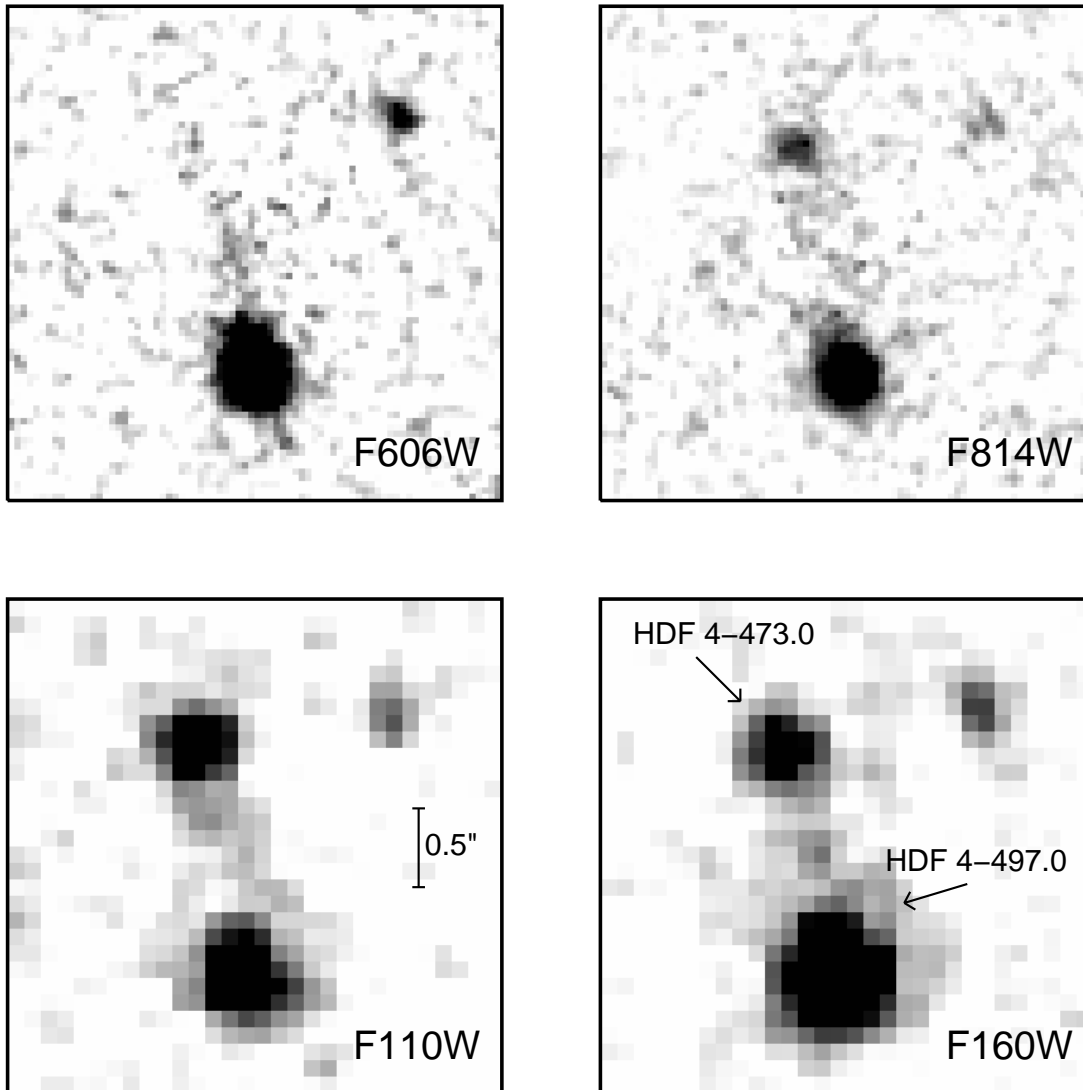


Fig. 1.— Mosaic around HDF 4-473.0 in the F606W ($\sim V$), F814W ($\sim I$), F110W ($\sim J$), and F160W ($\sim H$) passbands. AB $1''$ diameter aperture magnitudes are >29.4 , 27.1 , 26.6 , and 26.9 , respectively. 4-473 is located at $\alpha = 12^h 36^m 45^s 902$, $\delta = 62^\circ 11' 58'' 21$ (J2000). Images shown are $3''$ on a side. Bunker *et al.* (1998) have shown HDF 4-497.0 to be at $z = 2.80$.

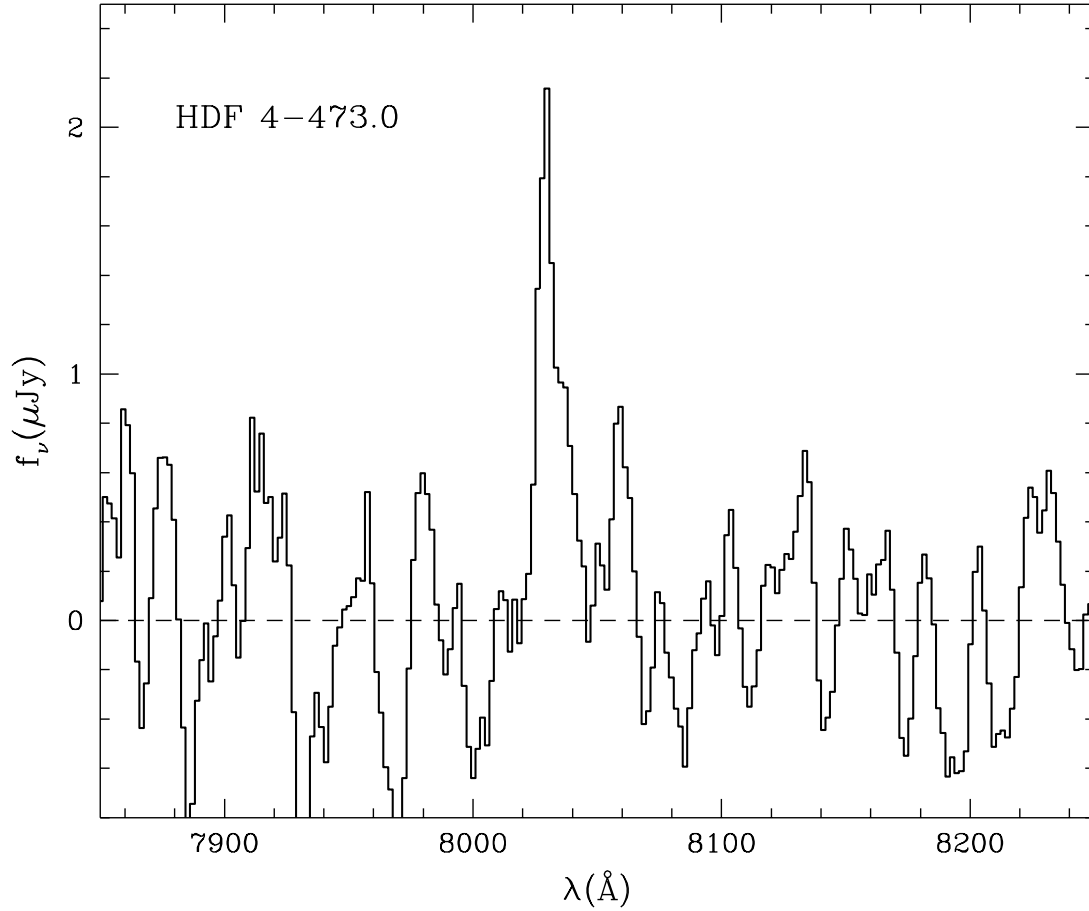


Fig. 2.— Spectrum of HDF 4–473.0 showing the emission line at 8029 Å. The asymmetric line profile and broad band colors are consistent with this being Ly α at $z = 5.60$. The total exposure time is 14,400 seconds, and the spectrum was extracted with a 1.7'' aperture. The spectrum has been smoothed using a 5-pixel boxcar filter.

Table 1. Predicted AB magnitudes for Higher Redshift Galaxies

| z | Flux ($\text{Ly}\alpha$) | F160W | F110W | F814W | F606W | K | F110W-F160W | F814W-F110W |
|------|-------------------------------|-------|-------|-------|-------|-------|-------------|-------------|
| 5.6 | $1.2\text{e-}17$ | 26.86 | 26.64 | 27.13 | 30.09 | 27.07 | -0.22 | +0.49 |
| 6.0 | $9.6\text{e-}18$ | 26.98 | 26.85 | 27.77 | 32.10 | 27.19 | -0.14 | +0.92 |
| 7.0 | $6.3\text{e-}18$ | 27.21 | 27.33 | 31.36 | — | 27.39 | +0.12 | +4.03 |
| 8.0 | $4.3\text{e-}18$ | 27.44 | 27.93 | — | — | 27.59 | +0.49 | — |
| 9.0 | $3.1\text{e-}18$ | 27.63 | 28.63 | — | — | 27.76 | +1.00 | — |
| 10.0 | $2.3\text{e-}18$ | 27.81 | 29.66 | — | — | 27.93 | +1.85 | — |